Viscosity of Polydimethylsiloxane Gum: Shear and Temperature Dependence from Dynamic and Capillary Rheometry

FRANK E. SWALLOW

Dow Corning Corporation, Barry CF63 2YL, United Kingdom

Received 26 March 2001; accepted 18 September 2001

ABSTRACT: The rheology of Dow Corning polydimethylsiloxane gum (PDMS/silicone gum) was studied over a time range of 10^{-2} to 10^{5} s^{-1} and a temperature range of 23–150°C using both capillary and dynamic rheometry. A low shear Newtonian region is observed at room temperature below 0.01 rad/s (increasing to 0.1 rad/s at 150°C) for which an Arrhenius activation energy for a viscous flow of 13.3 kJ/mol was determined. The Cox–Merz rule for merging of shear and complex viscosities is found to be valid up to 10 s^{-1}. Viscosity is found to be independent of temperature above 100 s^{-1}, where terminal power-law flow is encountered. This is exhibited in the dynamic data as equal plateau moduli for the various temperature curves. Gross wall slippage is seen in capillary flows above approximately 100 s^{-1}, corresponding to a stress value of 70–100 kPa. Slip-stick (spurt) flow is not observed. The viscosity data are best fitted by the Carreau–Yasuda model with a fitting parameter a of 0.7, a power-law index n of 0.05 (low because of slip effect), and a zero shear viscosity of 32 kPa s at 23°C. © 2002 Wiley Periodicals, Inc. J Appl Polym Sci 84: 2533–2540, 2002

Key words: silicone gum; polymer slip; polydimethylsiloxane; rheometry; Carreau–Yasuda relation; polysiloxanes; rheology; shear; silicones; visoelastic properties

INTRODUCTION

During 1998, the engineering group within the Dow Corning Corp. had need of shear viscosity data on high molecular weight silicone polymers (gums) for use in the design of processing equipment. Internal data were found to be limited in both shear rate and temperature range and data in the open literature were mainly concerned with zero shear viscosities[1,2] or lower molecular weight fluids[3] and could not readily be applied to the purposes of equipment design for commercial gums. The work most closely matched to Dow Corning gum was that on Rhône–Poulenc silicone fluids by El Kissi and Piau,[4,5] while the data on a Wacker Chemie fluid by Ohl and Gleissle[6] indicated the expected behavior and viscosity model-fit parameters, without providing crucial information on the molecular weight. Consequently, a short program of work was initiated to generate definitive rheological data for one of the company's gum products using capillary and dynamic rheometry.

EXPERIMENTAL

Materials

The material chosen for study was a commercial silicone gum from the Dow Corning Corp. (referred to as DC in this article). It is a vinyl end-blocked polysiloxane copolymer of the form CH_2═CH—

Journal of Applied Polymer Science, Vol. 84, 2533–2540 (2002)

$[(CH_3)_2SiO]_x$—$[(CH_2{=}CH)(CH_3)SiO]_y$—$CH{=}CH_2$ (where $x = 600$ and $y = 1$) with $M_w = 590{,}000$ and $M_w/M_n = 2.2$ (based on the polymer fraction). The bulk material contains approximately 1% w/w of the octamethyl cyclotetrasiloxane monomer and 6% w/w of larger cyclic species and has a maximum branching level of 25 ppm from trifunctional groups.

Capillary Rheometer

Capillary data were obtained using a Rosand capillary rheometer. Three circular, hardened steel rod dies were used, each having the same 16:1 L/D ratio: 32/2, 16/1, and 4/0.5 (dimensions in millimeters) with a flat-face entry profile (180°). Orifice dies (zero length) were used to determine the Bagley entrance losses, again at diameters of 2, 1, and 0.5 mm with an 180° entry profile.

To load the sample, gum was rolled into small lozenges and inserted into 15-mm diameter barrels. Each piece was packed down by manually ramming with the piston to ensure that no air was left trapped. Set points of 23, 80, and 150°C were used. The system attained a steady set-point temperature after approximately 10 min (checked by use of an independent thermocouple). After reaching the steady-state temperature, the crosshead was lowered manually until the material was ejected continuously from both long and short dies. A further 10-min rest was provided to allow the pressure to relax in the long die. (No further preloads or holds were requested within the software on start up.)

To avoid confusion in data interpretation that can occur where slip is present, no software correction factors were applied (e.g., Rabinowitch), information being collected on ram speeds and pressures above the dies from which shear rates and stresses were calculated using the standard equations. The apparent shear rate at the wall for the specific case of the Rosand with a 15-mm barrel and dies of diameter d (mm) is

$$\dot{\gamma}_{a\omega} = \frac{4Q}{\pi R^3} = \frac{30 \times \text{ram speed (mm/min)}}{d^3} \quad (1)$$

the stress at the wall is

$$\tau_\omega = \frac{\Delta P}{2}\frac{R}{L} \quad (2)$$

and the apparent viscosity is

$$\eta = \frac{\tau_\omega}{\dot{\gamma}_{aw}} \quad (3)$$

Dynamic Rheometer

The Rheometrics RDS2 Model of a controlled strain rheometer was used in the dynamic mode using either 25- or 50-mm parallel plates.

Sample Preparation

Approximately 1.1 g of gum was squashed between the 25-mm parallel plates (or 4.5 g on the 50-mm plates) to a thickness of 2.020 mm and allowed to rest for 2 min (by which time the normal stress had decayed to zero). The sample was then trimmed to match the edge of the plates and the thickness decreased to 2.000 mm followed by a further 2-min rest period.

Strain Dependence

A strain sweep was run at a frequency of 1 rad/s, which determined that the linear viscoelastic (LVE) region extended out beyond 70% strain. A series of frequency sweeps at various strain levels confirmed the independence of strain between 0.1 and 10% upon the frequency response between 0.5 and 500 rad/s. These findings suggested that a high strain value of 10% could be used to maximize the torque response, yet remain within the LVE region.

Test Repeatability

A frequency sweep was run on a series of five completely fresh samples loaded onto the 25-mm plates and a sixth run made using 50-mm plates. The runs included repeat tests on the same sample, varying levels of rest periods, and also a pretrain time sweep. Data overlap on fresh, repeat, or prestrained samples was almost perfect, indicating the reliability of the preparation technique and the sufficiency of the 2-min rest period, with no requirement for a prestrain (i.e., no thixotropy was detected).

Frequency Sweep

Given the findings on strain dependence, frequency response data were collected using either the 25- or 50-mm parallel plates at a strain of 10% and at temperatures of 23, 80, and 150°C. Data for the three temperatures were collected using the 25-mm plates in the frequency range 0.5–400

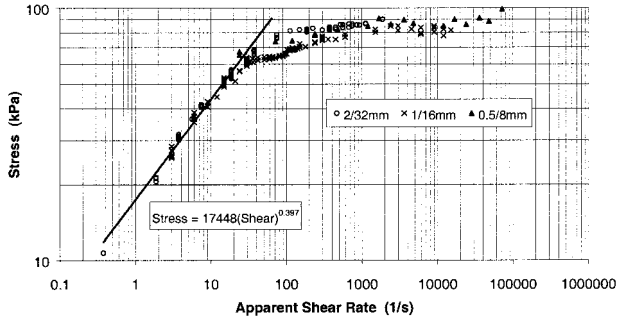

Figure 1 Stress versus apparent shear rate for three dies at room temperature.

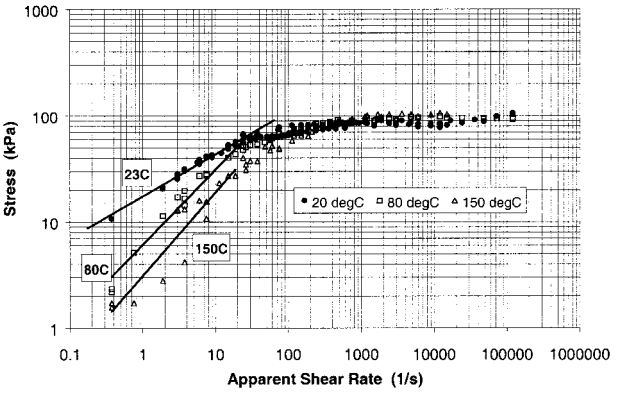

Figure 2 Stress versus shear: impact of temperature.

rad/s. The lowest-frequency, highest-temperature point gave a minimum torque of 1.8 g cm, just below the transducer limit of 2 g cm. All other points were within the transducer operating range.

The 50-mm plates were used to reduce the frequency down to 0.01 rad/s, giving a minimum torque of 7.8 g cm (maximum 1740 g cm) for the 23°C run. It was not possible to extract data for the higher temperatures because, at the long time period required for the low frequencies, the gum flowed out of the plates and sample integrity was lost.

RESULTS

Capillary Data

Stress and Viscosity

Figure 1 looks at the consistency of stress data between different dies for DC gum at 23°C. The dies appear to give consistent stress data, particularly in the non-Newtonian region below shear rates of 100 s^{-1}. Above this shear rate, the stress data appear to flatten and some discrepancies are seen between the dies.

The impact of temperature is shown in Figure 2. Below the critical shear rate of 100 s^{-1}, we see the expected dependence of stress upon the shear rate. Above this shear, we again see the stress curve flatten for each of the temperatures studied. Temperature appears to have no impact upon the stress and, thereby, viscosity, above this shear rate.

The temperature independence is also evident in the viscosity curve of Figure 3, where we see the three temperature curves merge as they enter the power-law flow region. Here, we also see evidence of a Newtonian plateau region at low shear, particularly for the higher temperatures, although there is considerable error in the data at the highest temperature (bottom of pressure transducer range). The overall power-law exponent (n) of 0.0525 (from gradient $m = -0.9475$, Fig. 3) is much lower than was expected.

Extrudate Quality

The character of the gum extrudate was monitored at room temperature and seen to vary with the extrusion rate. The surface effects generally followed those seen and photographically documented by El Kissi and Piau[4] for the Rhône–Poulenc BG gum. What may be termed as a "good-quality" extrudate, that is, that with a smooth, shiny surface with little die swell, was seen only at very low shear rates.

At a shear rate of approximately 5 s^{-1}, small ripples that created a matte (nonshiny) surface were visible. These ripples had grown into a distinct "saw-tooth" pattern by 15 s^{-1}, which had the appearance of a screw thread (i.e., the deforma-

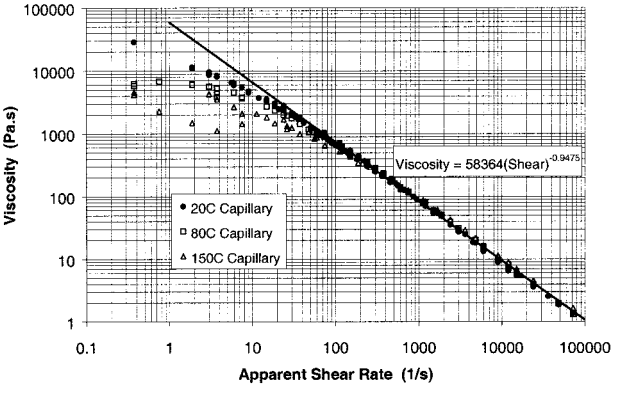

Figure 3 DC gum viscosity: impact of temperature.

tion was initiated at one point at the die exit and progressed around the die circumference).

By a shear rate of 30 s^{-1}, gross, yet periodic, deformations in flow that resembled flow pulsations became visible, with chaotic melt fracture occurring around 50 s^{-1}. It is interesting to note that melt fracture had occurred at the low shear rate of 50 s^{-1}, prior to the stress-flattening phenomenon that was seen at 100 s^{-1}.

Dynamic Data

The frequency response of dynamic viscosity for DC gum over the temperature range 23–150°C is shown in Figure 4. The plot may be compared with that obtained from capillary data (Fig. 3), in that we see a clear Newtonian region with zero shear viscosities and a merging of the temperature curves in the power-law region at higher frequencies. There is excellent agreement between the data for the 25- and 50-mm plates. The viscosity data were also compared and found to be in close agreement with several internal studies by other investigators on different rheometers in both the dynamic and continuous shear modes.

DISCUSSION

Capillary Data

The stress behavior of gum above a shear rate of 100 s^{-1} (in Figs. 1 and 2) requires explanation. There is a sudden transition from normal non-Newtonian flow to an almost flat-stress region that is apparently independent of temperature.

In their work, with Rhône–Poulenc gums, El Kissi and Piau[4] reported similar types of behavior, with gums above a critical molecular weight exhibiting a phenomenon known as spurt flow. (Specifically, this is expected to occur for polymers

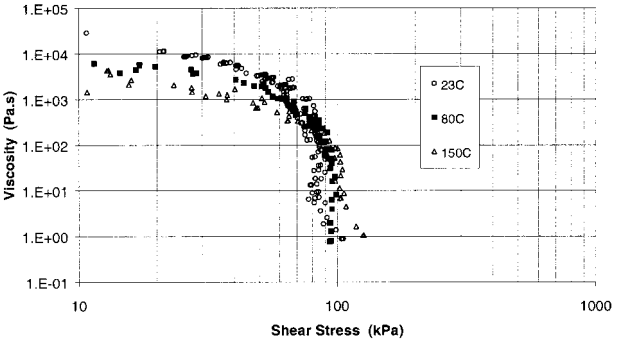

Figure 4 Viscosity versus shear stress.

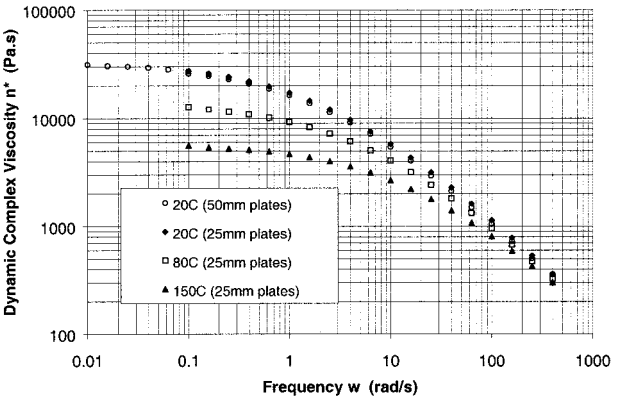

Figure 5 Dynamic (complex) viscosity of DC gum.

with a ratio $M_w/M_c > 16$, where M_c is the critical weight for entanglement.) This spurt behavior is well documented in the literature for other polymers (e.g., Adewale and Leonov[7]) and has also been observed by the present author for silica-filled silicone rubbers (unpublished). Based upon El Kissi and Piau's findings, we would expect, although do not see, a classical spurt flow in our DC gum (for which $M_w/M_c = 20$). Further, there was no evidence of oscillation in the pressure above the die and there was no visible extrudate flow surging (as would be expected in spurt flow).

The room-temperature flow behavior above 100 s^{-1} should therefore be seen more as a gross slippage of the polymer at the critical stress of 70–90 kPa (in common with other polymers), rather than the "slip-stick" phenomenon of spurt flow. The variation of slip with temperature is shown in the viscosity versus stress curves of Figure 4, where we see an increasing reluctance to slip as the temperature increases.

There may be some evidence of a return to a more normal flow behavior at higher shear rates with the last few data points in the 23 and 150°C stress curves of Figures 1 and 4 showing a consistently increasing stress level, outside the stress band of lower rates. Ito and Shishido[8] reported an upper Newtonian region for PDMS above rates of 10^5 s^{-1}; hence, we might expect some upward movement of the stress curve around 10^4 s^{-1}. Equipment limitations prevented exploration above this rate in this study. The unexpectedly low value of 0.05 for the power-law index is therefore attributed to this high shear-slip phenomenon.

Dynamic Data

The behavior of the complex viscosity may be seen in Figure 5. The independence of temperature

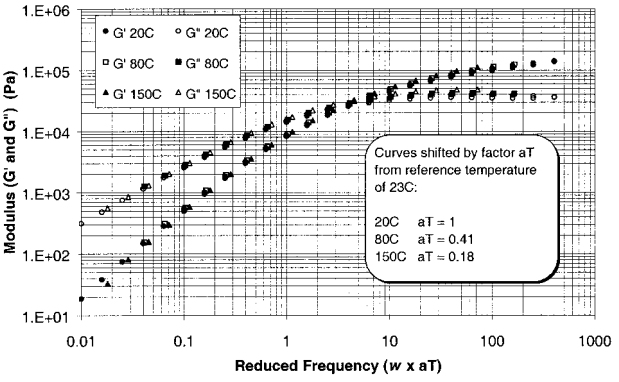

Figure 6 DC gum: time–temperature superposition of moduli.

upon viscosity seen in the capillary data above 100 s^{-1} is mirrored here as the complex modulus enters the plateau region above a frequency of 100 rad/s. The elastic and viscous loss moduli for the three temperatures are shown in their shifted forms in Figure 6 (fitted using a least-squares technique with 23°C as the reference temperature). [Note: The shift factors derived from the dynamic moduli are essentially identical to those derived from the zero shear viscosities of the Yasuda models (below) because these are heavily influenced by the dynamic data at low frequency.]

Application of Cox–Merz Rule

The Cox–Merz[9] rule allows us to combine viscosity data from dynamic and flow rheological studies by equating the frequency (rad/s) with the shear rate (s^{-1}) and overlaying the dynamic complex and capillary shear viscosities. The data from dynamic and capillary rheometry on DC gum were found to follow the Cox–Merz rule well for all temperatures, up to a rate of approximately 10 s^{-1}. Figure 7 shows the combined data for DC gum at 23°C, including curve fits to both a Carreau[10] and the more representative Carreau–Yasuda[10,11] model—

$$\text{Carreau:} \quad \eta = \eta_0[1 + (\lambda\dot{\gamma})^2]^{[(n-1)/2]} \tag{4}$$

$$\text{Yasuda:} \quad \eta = \eta_0[1 + (\lambda\dot{\gamma})^a]^{[(n-1)/a]} \tag{5}$$

where η_0 is the zero shear viscosity; n, the power-law exponent; a, a fitting parameter, and λ, a characteristic time of the material (specifically, the reciprocal of the intercept between the power-law line and the zero shear viscosity). The Carreau model is seen as a specific case of the Yasuda model where $a = 2$.

The Yasuda model parameters of η_0 and a were determined by minimization of residuals, the parameter n being derived from the capillary power-law exponent, with λ following from knowledge of η_0, n, and K_1 (the power-law preexponent in Fig. 3). For DC gum at 23°C,

$$\eta_{(23)} = 32000[1 + (0.53\dot{\gamma})^{0.7}]^{-1.3536} \text{ Pa s} \tag{6}$$

Comparison to the Literature

A comparison can made with the data reported by Piau et al.[5] on Rhône–Poulenc high-viscosity sil-

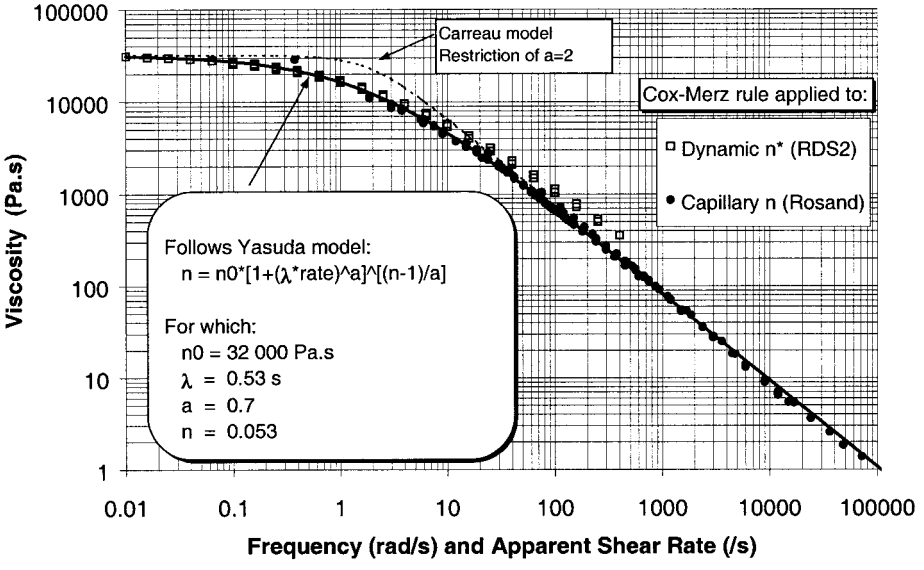

Figure 7 Model fitting to DC gum at room temperature.

Table I Properties and Yasuda Model Parameters for Comparable Gums

PDMS	M_w (10^3 g/mol)	M_w/M_n	Branching (ppm)	Predicted η_0 [(eq. (7)] (10^3 Pa s)	Measured η_0 (10^3 Pa s)	λ (s)	a	n
LG1	418	3.2	0	17.0	15.0	0.30	0.31	0.10
LG5	490	1.9	0	29.8	22.0	—	—	—
BG	428	2.9	50	18.5	55.0	3.0	0.3	0.22
BW400	—	—			11.0	0.14	0.65	0.04
DC	590	2.2	25	57.4	32.0	0.53	0.70	0.05

icone fluids. The fluids LG1 and LG5 (reported as experimental and commercial fluids, respectively) would appear to be closest to the DC gum, having similar molecular weights and polydispersity (Table I). BG is an experimental material with greater dispersity and more branching (Table I). Unfortunately, no information was disclosed on the volatile content of these materials. Piau et al. used a (temperature-modified) relationship based on the findings of Kataoka and Ueda[1] for the dependence of zero shear viscosity of silicones upon molecular weight (at 23°C):

$$\eta_0 = 2.44 \times 10^{-16} \times M_w^{3.53} \quad \text{for } M_w > 55{,}000 \quad (7)$$

The equation greatly overestimates the viscosity of the DC gum (Table I) and underpredicts the BG gum. The known volatile content of the DC gum and the branching present in the BG gum may be valid causes for these discrepancies. The reported Yasuda parameters enable construction of viscosity curves for LG1, BG, and DC fluids for comparison (Fig. 8).

Piau et al.[5] suggested that the Cole–Cole plot may be a means of qualitatively detecting branching in these polymers, such that branched siloxanes may deviate from a circular arc. An investigation of the Cole–Cole plot for repeat measures on the DC gum (Fig. 9) reveals a circular arc (with some repetition error at lower frequencies—right-hand arc), but with no evidence of any deviation—a flattening of the left-hand arc in Piau's work (Piau,[5] Fig. 2)—that could be attributed to the 25-ppm branching known to be present in the Dow Corning material.

Piau et al. also made use of the Yasuda model for the Rhône–Poulenc siloxanes (Piau et al.,[5] Table II) where they found the fitting parameter a to be consistently around 0.3 and a power-law index n varying between 0.10 and 0.22. While the value of a is somewhat lower than the 0.7 found in this present study, the power-law index is close to that of 0.18 found by Lee et al.[3] for lower-viscosity polysiloxanes.

In their work on viscoelastic suspensions, Ohl and Gleissle[6] reported the Yasuda parameters for

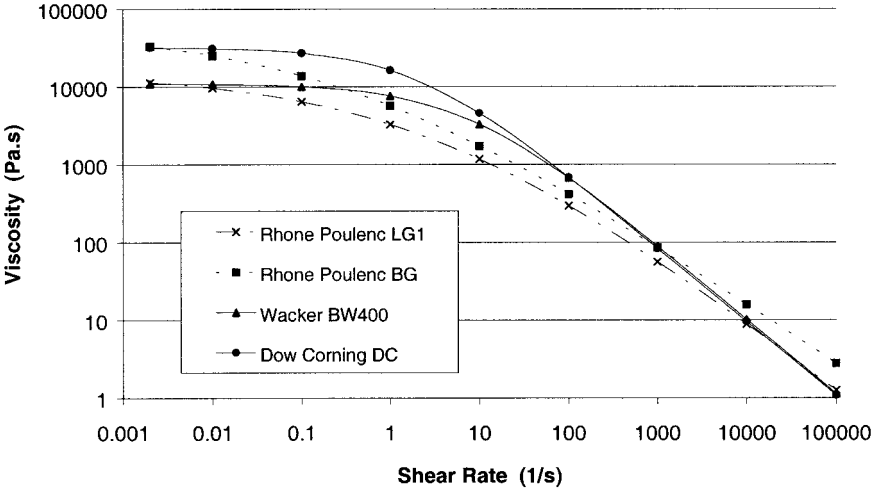

Figure 8 Yasuda model curves for comparable gum fluids.

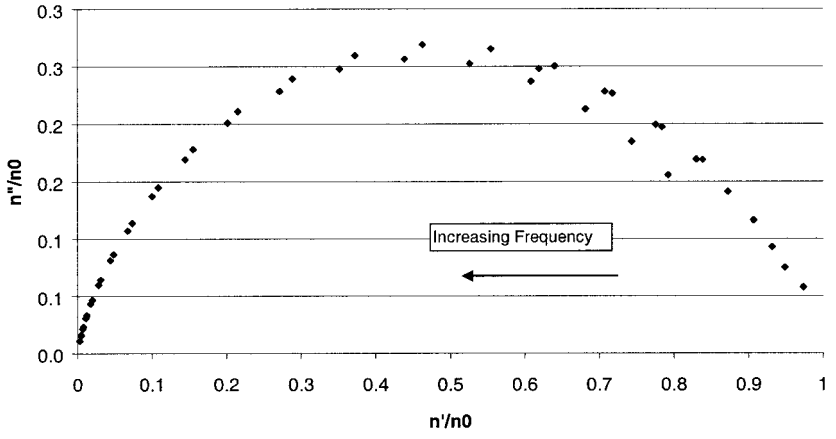

Figure 9 Cole–Cole diagram for DC gum.

the pure silicone fluid BW400 from Wacker–Chemie. Although no molecular weight details were given, the zero shear viscosity of 11 kPa s and the small characteristic time of 0.14 s would suggest a gum-type polymer with a low volatile content. In particular, the fit parameter a of 0.65 and power-law index n of 0.04 are remarkably close to that of the Dow Corning gum.

Temperature Impact

Figure 10 combines the complete data sets from the capillary and dynamic testing in the present study, together with the Yasuda model curve fits at all three temperatures (Table II). The fitting parameter a in the Yasuda model was found to be 0.7 for all three temperatures. The Yasuda equation for each temperature thus collapses into a function of the zero shear viscosity alone (for a given power-law behavior), suggesting a master equation for the shear and temperature response (see below).

DC Gum Zero Shear Viscosities

The zero shear viscosities (for DC gum) were found to follow the expected Arrhenius behavior, known here specifically as the Eyring[12] relationship:

$$\eta_0 = Ae^{E/RT} \tag{8}$$

where R is the universal gas constant (R = 8.3143 kJ kmol^{-1} K^{-1}). Note that, as we are far above the 150 K T_g of polydimethylsiloxanes, use of the WLF relationship is not appropriate. The activation energy for viscous flow can be calculated to be E = 13.3 kJ/mol, for which E/R (the temperature coefficient) is approximately 1600 K and the pre-exponent A = 136 Pa. This activation energy compares well with that found by a recent internal investigator (Hannington, unpublished) for low-viscosity siloxanes (E = 13.1 kJ/mol), although both findings are somewhat lower than the typical values of 14–16 kJ/mol reported in much earlier internal work by Polmanteer (an extension of ref. 3) and externally by Wang and Porter.[12]

DC Gum Viscosity Master Equation

As noted earlier, given the same power-law behavior and value of the Yasuda fitting parameter a, the Yasuda models at the various temperatures

Table II Yasuda Model-fit Parameters for DC Gum

Temperature (°C)	Zero Shear Viscosity η_0 (Pa s)	Characteristic Time λ (s)	Fitting Parameter a	Power-law Index n
23	32000	0.53	0.7	0.0525
80	13000	0.21	0.7	0.0525
150	6000	0.09	0.7	0.0525

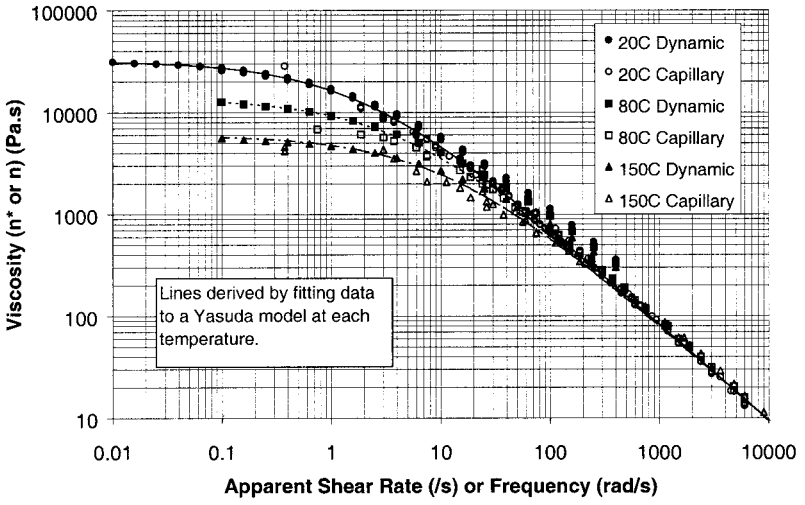

Figure 10 Temperature impact upon viscosity of DC gum.

collapse into a dependency upon the zero shear viscosity, which, in turn, is a function of the temperature. If we also recognize that the characteristic time λ (derived from the intercept of the power-law curve with the zero shear viscosity) must also be a simple function of temperature, then we can rewrite the Yasuda model as

$$\eta = \eta_{0(\mathrm{ref})} a_t [1 + (\lambda_{\mathrm{ref}} a_t \dot{\gamma})^a]^{(n-1)/a} \tag{9}$$

where $\eta_{0(\mathrm{ref})}$ is the zero shear viscosity; λ_{ref}, the characteristic time at a chosen reference temperature; and a_t, the shift factor at a given temperature:

$$a_t = e^{E/R(1/T - 1/T_{\mathrm{ref}})} = e^{1600(1/T - 1/296)} \tag{10}$$

For our specific case of the DC gum with a reference temperature of 23°C, this generates the general equation for viscosities between temperatures of 23 and 150°C and shear rates of 0.01 and 10^5 s^{-1} as

$$\eta = 136 e^{1600/T} [1 + (0.00225 e^{1600/T})^{0.739} \dot{\gamma}^{0.7}]^{-1.354} \text{ Pa s} \tag{11}$$

CONCLUSIONS

The Cox–Merz relationship was found to hold for high-viscosity polydimethylsiloxane (silicone) gum. A low shear Newtonian plateau is observed below 0.01 rad/s at room temperature (increasing to 0.1 rad/s at 150°C), for which an "activation energy" for viscous flow of 13.3 kJ/mol was determined. The stress/shear curves (23–150°C) are seen to merge at 100 s^{-1}, above which severe shear thinning is observed with an apparent power-law index of 0.053. This severe shear thinning may be caused by wall slippage and corresponds to the shear-stress region of 70–100 kPa in which other polymers are known to show slip behavior. A Yasuda model fitted to the combined dynamic and capillary data best describes the shear-viscosity curve.

REFERENCES

1. Kataoka, T.; Ueda, S. J Polym Sci A-1 1967, 5, 3071.
2. Friedman, E. M.; Porter, R. S. Trans Soc Rheol 1975, 19, 493–508.
3. Lee, C. L.; Polmanteer, K. E.; King, E. G.J Polym Sci 1970, 8, 1909–1916.
4. El Kissi, N.; Piau, L. M. J Non-Newtonian Fluid Mech 1990, 37.
5. El Kissi, N.; Piau, J. M.; Attane, P.; Turrel, G. Rheol Acta 1993, 32, 293–310.
6. Ohl, N.; Gleissle, W. J Rheol 1993, 37, 381–406.
7. Adewale, K. P.; Leonov, A. I. Rheol Acta 1997, 6, 110–127.
8. Ito, Y.; Shishido, S. J Polym Sci 1973, 11, 2283.
9. Cox, W. P.; Merz, E. H. J Polym Sci 1958, 28:619–622.
10. Carreau, P. J.; DeKee, D. C. R.; Chhabra, R. P. Rheology of Polymeric Systems; Hanser: Munich, 1997.
11. Dealy, J. M.; Wissbrun, K. F. Melt Rheology and Its Role in Plastics Processing; Van Nostrand Reinhold: New York, 1990.
12. Wang, J.; Porter, R. S. Rheol Acta 1995, 34, 496–503.